BOLLETTINO DI GEOFISICA TEORICA ED APPLICATA VOL. XXXV, N. 137-138 - MARCH-JUNE 1993

R. GELETTI [1], M. PIPAN [1] and A. VESNAVER [2]

SIGNAL/NOISE RATIO ENHANCEMENT OF SEISMIC PROFILES IN THE ROSS SEA (ANTARCTICA)

Abstract. Several seismic profiles recorded by the OGS in the Ross Sea (Antarctica) have been processed and interpreted. Attenuation of the strong multiple reflections, due to the frozen sea bottom, affecting the seismic records is the primary objective of this study. Various processing techniques were applied to improve the signal/noise ratio, such as weighted stack and iterated pre-stack *f-k* domain filtering, and the results obtained are reported and discussed. Furthermore, a new technique is introduced: pre-stack *f-x* deconvolution.

INTRODUCTION

Reconstruction of the crustal conditions of the Antarctic continental shelf is mainly based on the interpretation of geophysical data and, in particular, of large multichannel seismic reflection datasets. Extensive geophysical exploration programmes have been completed by the OGS in the Ross Sea area (1987/88, 1988/89) as a part of the Italian National Programme of Antarctic Researches, leading to the acquisition of more than 9000 km of seismic lines. The following table illustrates the acquisition parameters of the OGS Antarctic seismic surveys.

SEISMIC LINES - ACQUISITION			
Ship	OGS - Explora	Trace spacing	25 m
Period of acquisition	Jan-Feb 1988/1989	Shotpoint spacing	75 m
Source	Air-gun	Number of traces	96 (120)
Sampling interval	4 ms	Fold	16 (30)
Record length	24 sec	Streamer length	2400 m (3000 m)
Values in brackets ( ) refer to the second geophysical cruise (1989)			

The results of processing part of the seismic dataset by specific techniques for *signal-to-noise* ratio enhancement are illustrated by this paper. Two profiles are considered in particular here, IT89A25 and IT88A06, denoted also as lines A and B, respectively.

The Ross Sea is an epicontinental basin situated along the Pacific sector of Antarctica. The sea-bottom topography is characterized by rugged ridges interlaced with rather flat areas that represent minor depocenters of irregular shape. The combined effects of isostasy and gla-

Manuscript received September 3, 1992; accepted January 15, 1993.

[1] Istituto di Geodesia e Geofisica, University of Trieste, Via dell'Università 7, 34123 Trieste, Italy.

[2] OGS, Osservatorio Geofisico Sperimentale, P.O. Box 2011, 34016 Trieste, Italy.

cial erosion produce a characteristic landward gradient of the shelf within the basin. As an epicontinental sea, the average depth is notable; but from the seismic exploration point of view, the mean values around 500 meters represent a rather shallow water environment. This together with the strong reflectivity of the sea-bottom, probably connected to the widespread presence of permafrost along the top of the sedimentary sequence, generates strong multiple reflections which affect the whole span of the seismic record, interfering with all the primaries, from the shallow to the deepest horizons (Fig.1 and 2).

For the interpretation, attenuation of the multiple reflections in the deep part of the seismic sections is a crucial problem. An understanding of the deep crustal conditions in the Ross Sea area is of the utmost scientific interest due to the particular position and characteristics of this basin. The Ross Bay is part of a large depression which stretches from the Atlantic to the Pacific Ocean, thus separating the eastern and the western parts of the Antarctic continent. The basin is the result of a rifting which started in the late Mesozoic, as a probable consequence of the first phases of the Gondwana breakup, and it is still active in the westernmost part of the Bay. During this process, large systems of normal and strike-slip faults developed and the continental crust has thinned considerably throughout the basin. A great deal of important information for the reconstruction of the rifting process, for the analysis of the relationships between West and East Antarctica, and for the possible interpretation of seismic horizons corresponding to the deepest crustal discontinuities (Conrad, Moho) is expected from the processing of the Antarctic seismic data. The present study concentrates on the improvements obtained at and below the basement level through the application of a properly designed processing sequence.

ITERATED PRE-STACK F-K FILTERING

F-k domain filtering is one of the most powerful tools for attenuating multiple reflections. The method exploits their different velocity trends with respect to that of the primaries. Looking at a velocity spectrum (Fig.3a), the coherency peaks corresponding to the velocity function of multiples can be very easily identified, unlike those of primaries, which are much weaker.

Correcting the normal moveout of multiples, the undesired signals become sub-horizontal and can be removed by a reject filter in the *f-k* domain. As a first test, an egg-shaped reject band was designed in order to achieve an improvement of the filter impulse response (March and Bailey, 1983). The filtered section (Fig.4) shows a slight enhancement about the basement depth when compared with the original stack section (Fig.1). The limited effects of this type of *f-k* filter is most likely due to the simultaneous action on the primary and multiple reflections, due to the considerable width of the reject band about the maximum curvature zone of the filter.

A noticeable improvement is obtained through the application of a narrow filter with straight borders. The filter shape is a fan identified by two angles, which correspond to the lower and upper dip that are to be removed. Practical experience demonstrates that the band-pass width is a rather critical choice: if it is too small, noticeable multiple residuals are left; if it is too wide, the desired signal may be corrupted by the filtering itself or by its side effects. In the considered cases, the events with a slope between - 7 and 7 degrees in line A (Fig.5) were filtered out. In Fig.5b some low-amplitude signal with limited lateral continuity is hardly detectable.

After a removal of first order water bottom multiples, the second order ones were still present in the data. A possible approach to eliminating them was by a significant widening of the cut-off fan in the *f-k* domain. This choice, though cheaper than others, was discarded because of its excessive impact on the waveforms, which would have thus been distorted and blurred to a certain extent. We preferred to iterate the previous procedure, using the same filter shape and the velocity function of the second multiple train. Due to their late arrival time, we did not have to remove other higher order multiples.

In Fig.3b we can see that the velocity spectrum computed using the pre-stack *f-k* filtered traces contains no more of the low velocity coherency peaks which, due to their higher energy, hid the lower part of the primary velocity function. We were able to estimate a better stacking velocity in this way. Figs. 6 and 7 display the seismic stacked sections thus obtained, which allow us to distinguish several interesting deep primaries. Unfortunately, some filtering side effects can be noticed, particular in Fig.7, where linear dipping interference has been generated at large offsets. Muting such offsets achieves a noticeable reduction of this filtering noise, but reduces also its effectiveness at the same time. A satisfying solution to this drawback (a post-stack weighted mix) will be discussed later. Considerable improvements are introduced in both the shallow and deep part.

Some deep reflections are now clearly interpretable: we emphasize the presence of deep primaries between 7 and 8 s (Fig.6b). On the basis of structural models of the area obtained from the integrated interpretation of geophysical and geological data (Finetti et al., this monograph), we can identify this reflector with the Moho discontinuity with a high degree of confidence.

The good results obtained by iterated *f-k* filtering are computationally much more expensive than those of weighted stack or predictive deconvolution. On the other hand, an advantage of *f-k* filtering over these other methods is that it can be successfully applied under a much larger set of structural conditions. In fact, whilst predictive deconvolution (in time as well in the τ-p domain) works best if a regular periodicity is present in the multiple arrival times, prestack *f-k* domain filtering requires only an adequate moveout correction for the complexity of the considered structures. This means that the conventional hyperbolic moveout correction will be sufficient for flat layers, while dipping and curved reflectors will require either a preliminary moveout removal or a non-hyperbolic moveout correction (for example, a model-driven ray tracing).

WEIGHTED STACK

Conventional stack and stacking velocity analysis rely on the fact that often the earth's crust structure does not differ too much from the simple model formed by homogeneous horizontal layers. In this case, the traveltime curve of the reflected events can be well approximated by an hyperbolic function, i.e. the normal moveout. Most profiles recorded in the Ross Sea do not display very complex structures (such as salt domes or diapirs) which would suggest an 'ad hoc' processing procedure, such as the dip moveout removal or a pre-stack depth migration. Nevertheless, the image quality obtained with only accurate stacking velocity analyses and subsequent conventional stack is still somewhat confused in the deepest part (Fig.1). The classical and cheapest techniques typically used to reduce the long path multiples, such as gapped deconvolution, achieved only modest results.

The main cause of blurring in the seismic section is the interference between multiples and their residuals with the primaries from the deep reflectors. The sum of the out-of-phase but strong signals of multiples is larger than the in-phase stacked arrivals of the weaker primaries. In particular, at the nearest offsets, where the moveout curve is rather flat, the dereverberation effect of conventional stack is almost absent. For this reason, a time- and offset-varying weighting of the traces to be stacked is an effective tool to improve the *signal-to-noise* ratio in the lower part of the seismic section. Fig. 8 illustrates the result of a weighted stack of the *f-k* filtered CDP: both the basement and the deep reflector are more clearly interpretable and the overall presence of multiple reflection has been reduced. In the uppermost part of data, where only primaries or short path reverberations are present, the weighting function is almost flat with respect to the offset. For later arrivals, the weights have been estimated by proper mute scans. In Fig.9 an example of the selected weighting functions is depicted.

An advantage of the weighted stack is its low computational cost with respect to other techniques for multiples attenuation, such as τ-p domain deconvolution or pre-stack *f-k* domain filtering. On the other hand, it is not so effective, as we will see in the next section.

PRE-STACK F-X DECONVOLUTION

The *f-x* deconvolution was introduced by Gulunay (1986), and has become in the course

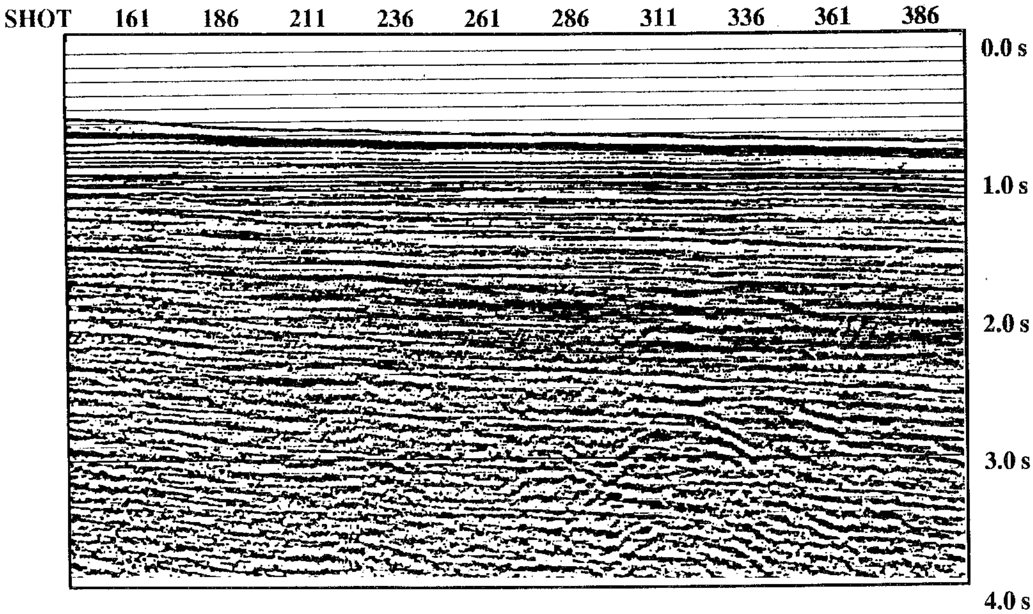

Fig. 1a — Line IT89A25: stack section after standard processing (shallow part).

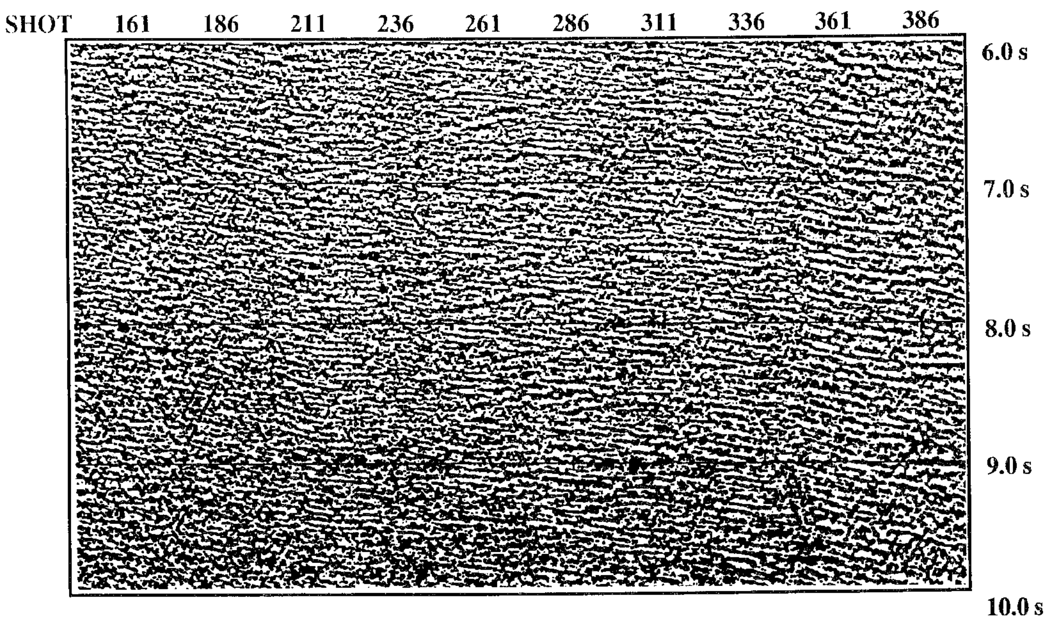

Fig. 1b — Line IT89A25: stack section after standard processing (deep part).

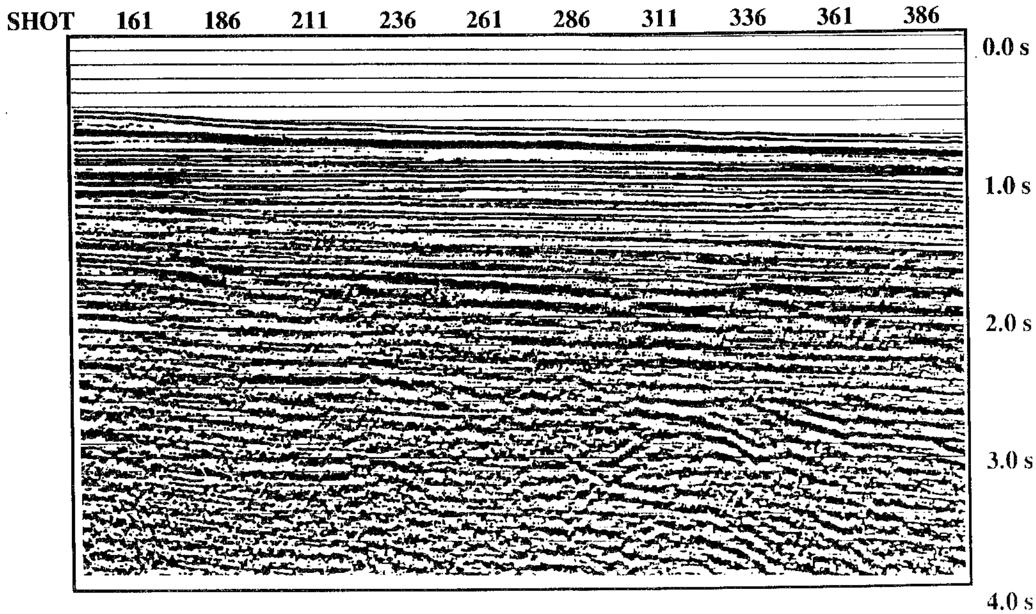

Fig. 2a — Line IT89A25: stack section after the application of an egg shaped fk filter before stack (shallow part).

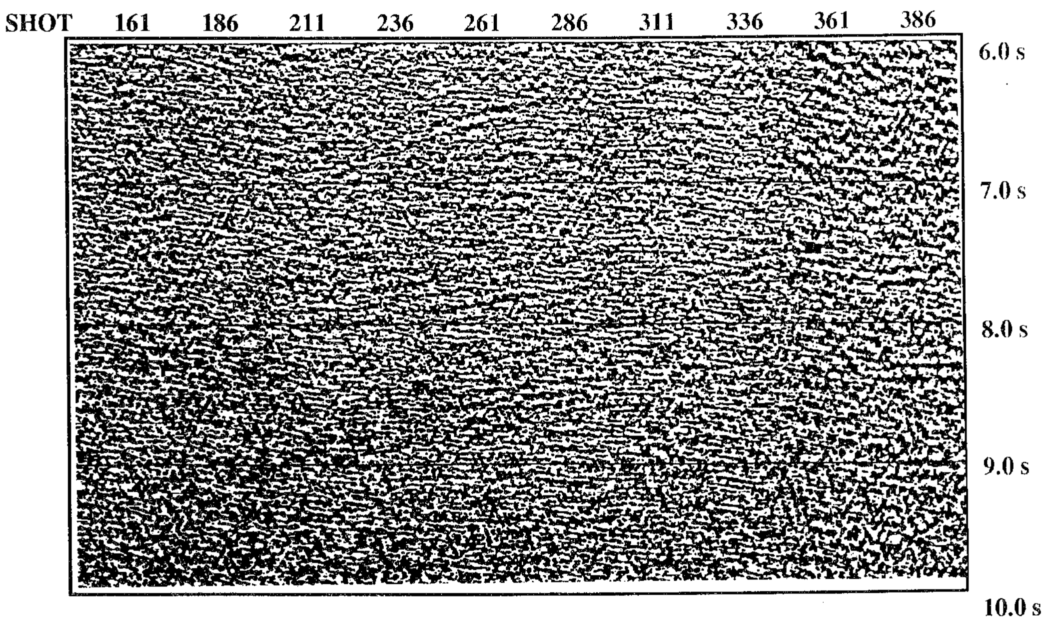

Fig. 2b — Line IT89A25: stack section after the application of an egg shaped fk filter before stack (deep part).

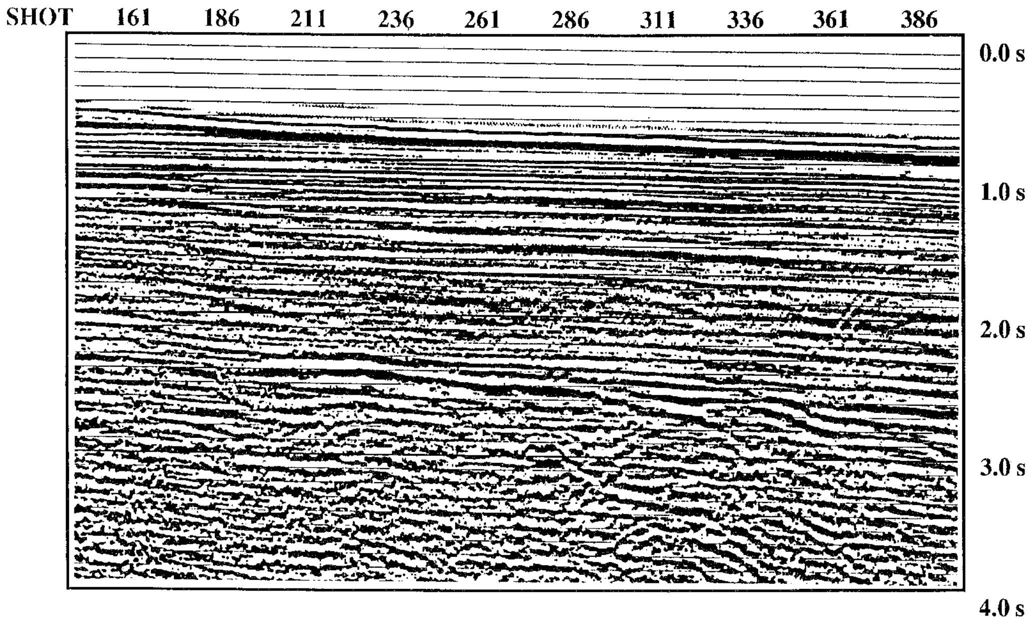

Fig. 3a — Line IT89A25: stack section after the iterated application of fk fan filters before stack (shallow part).

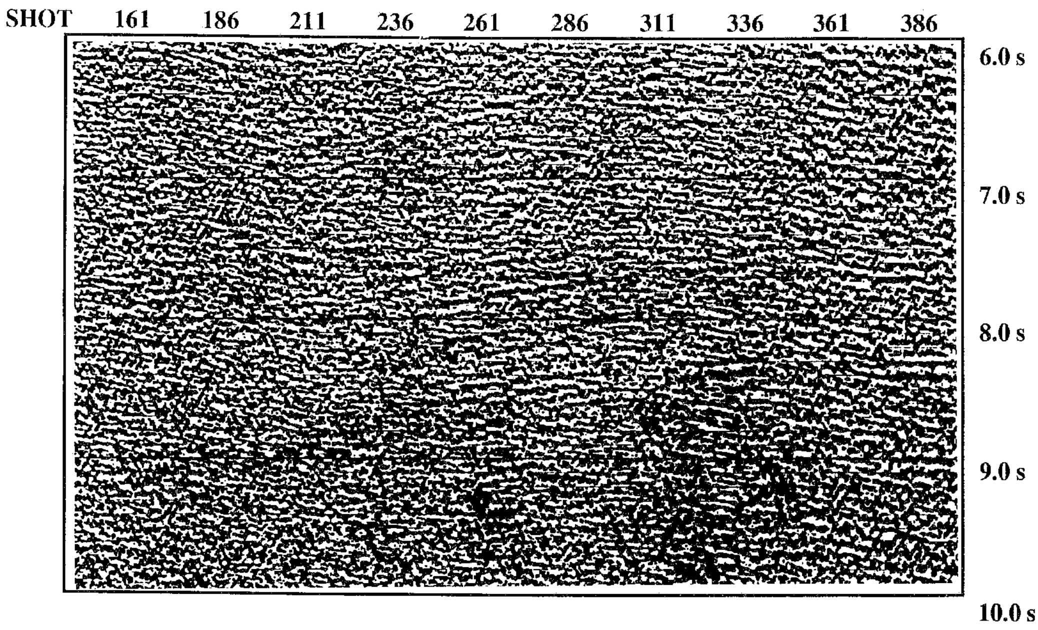

Fig. 3b — Line IT89A25: stack section after the iterated application of fk fan filters before stack (deep part).

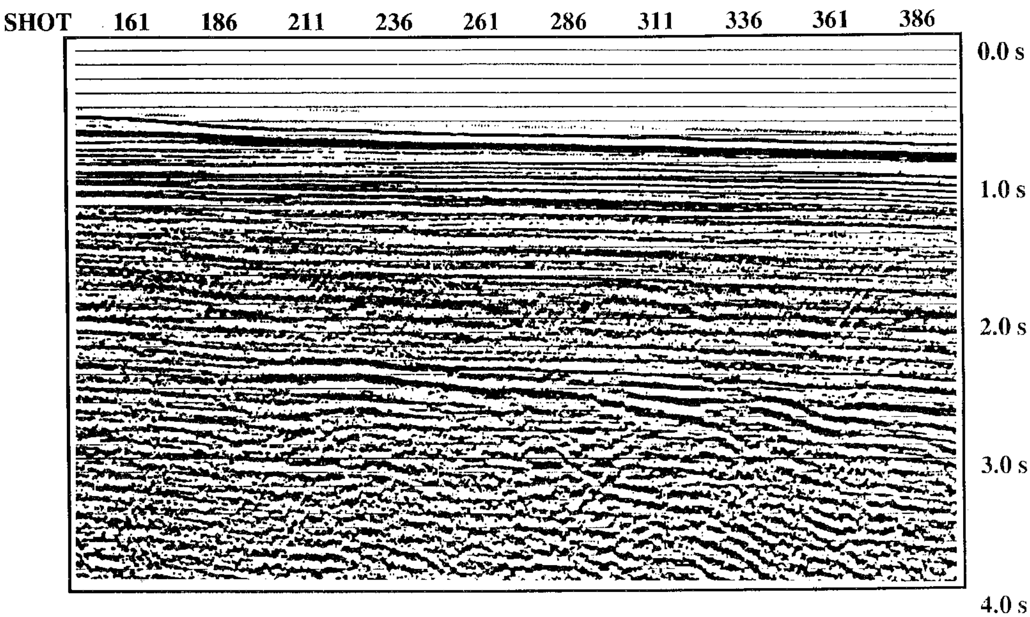

Fig. 4a — Line IT89A25: stack section after iterated fk filtering before stack and weighted stack (shallow part).

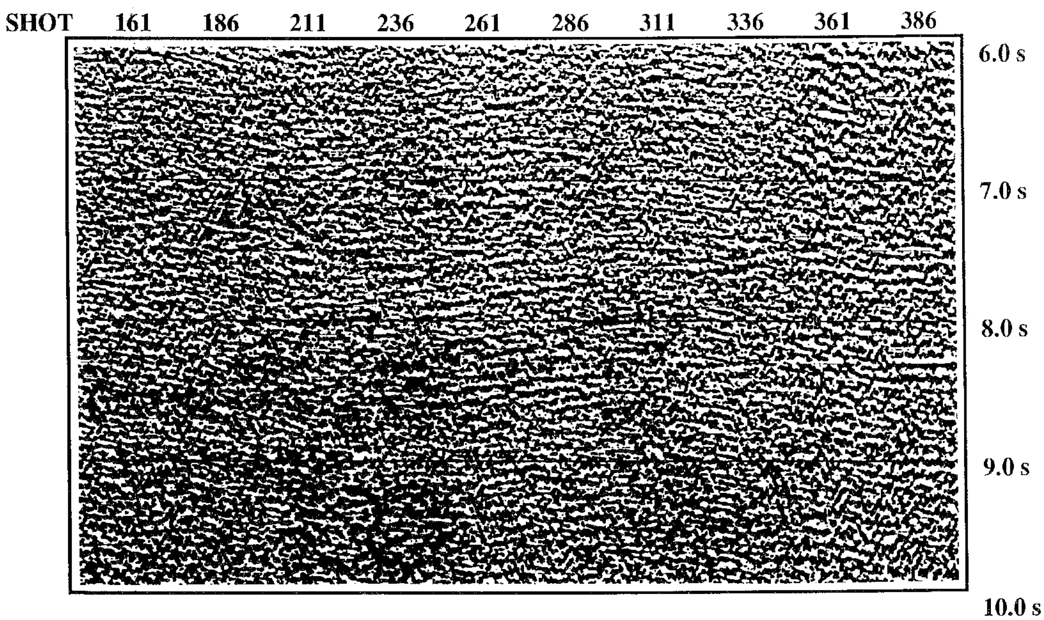

Fig. 4b — Line IT89A25: stack section after iterated fk filtering before stack and weighted stack (deep part).

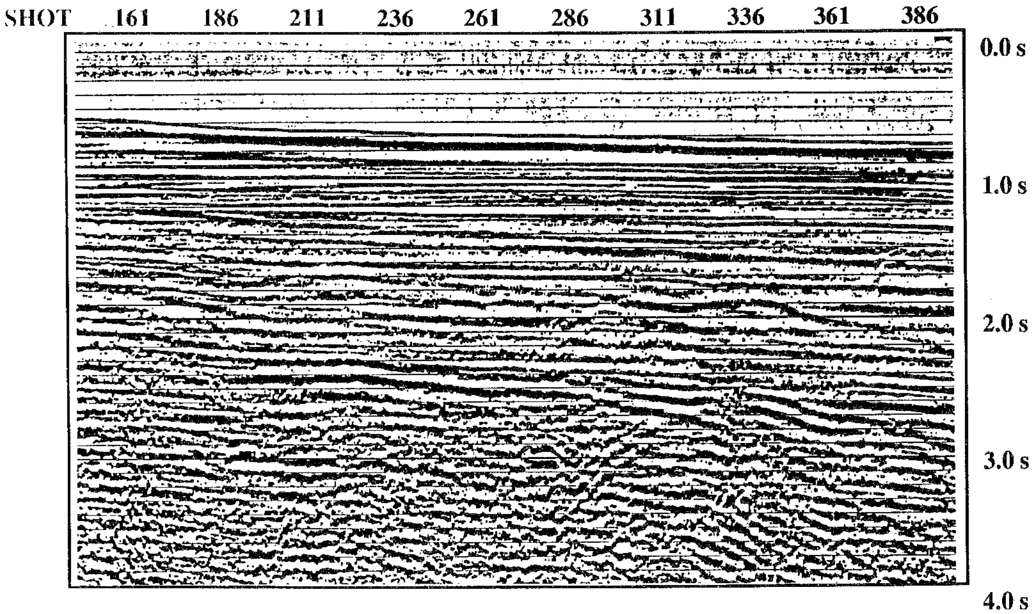

Fig. 5a — Line IT89A25: stack section after iterated fk filtering before stack (shallow part).

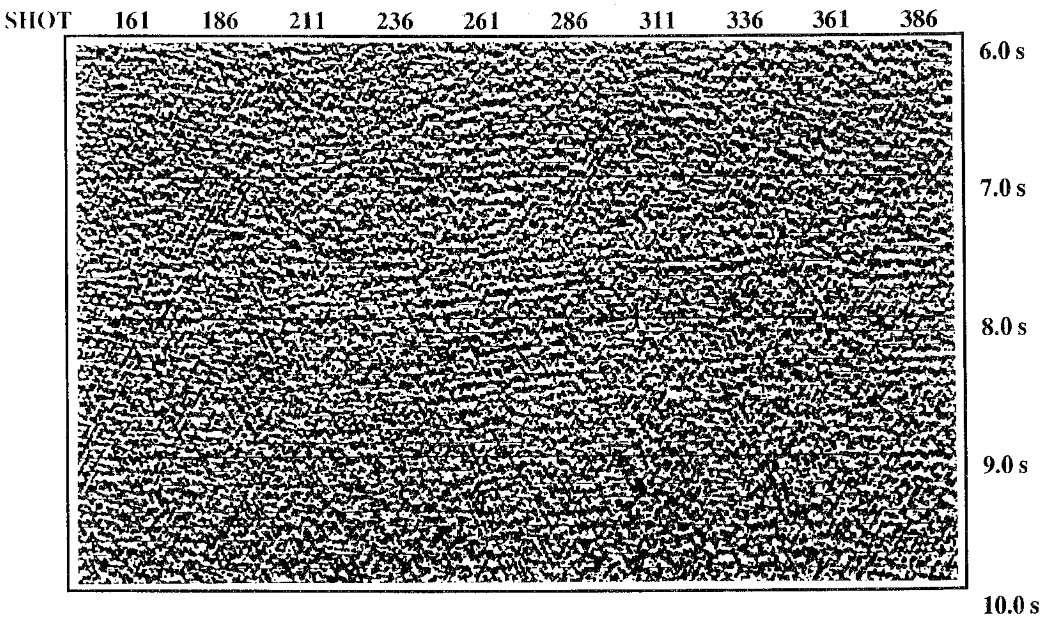

Fig. 5b — Line IT89A25: stack section after iterated fk filtering before stack (deep part).

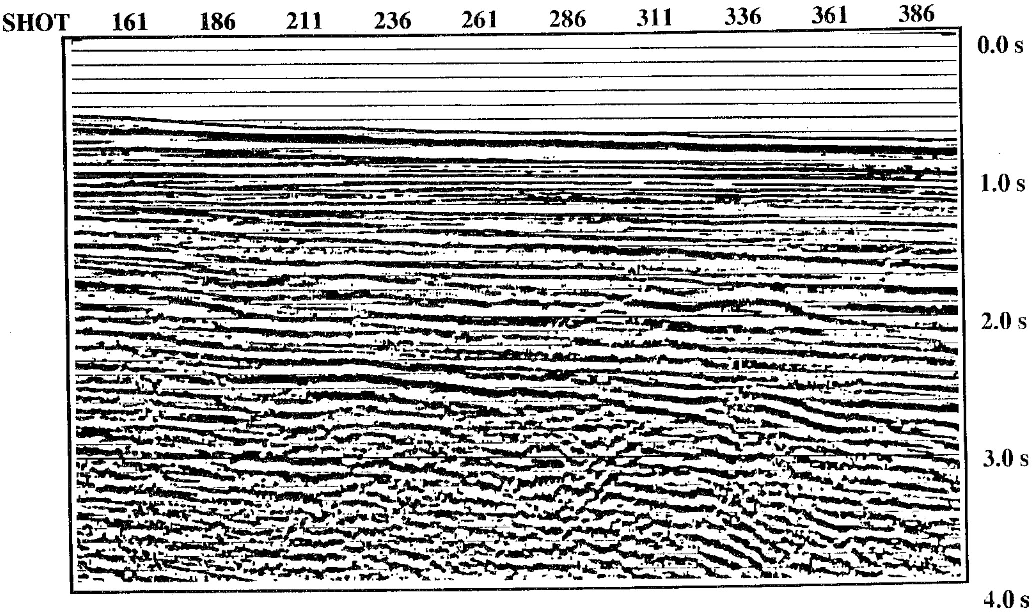

Fig. 6a —Line IT89A25: stack section of Fig. 5 after fx-deconvolution (shallow part).

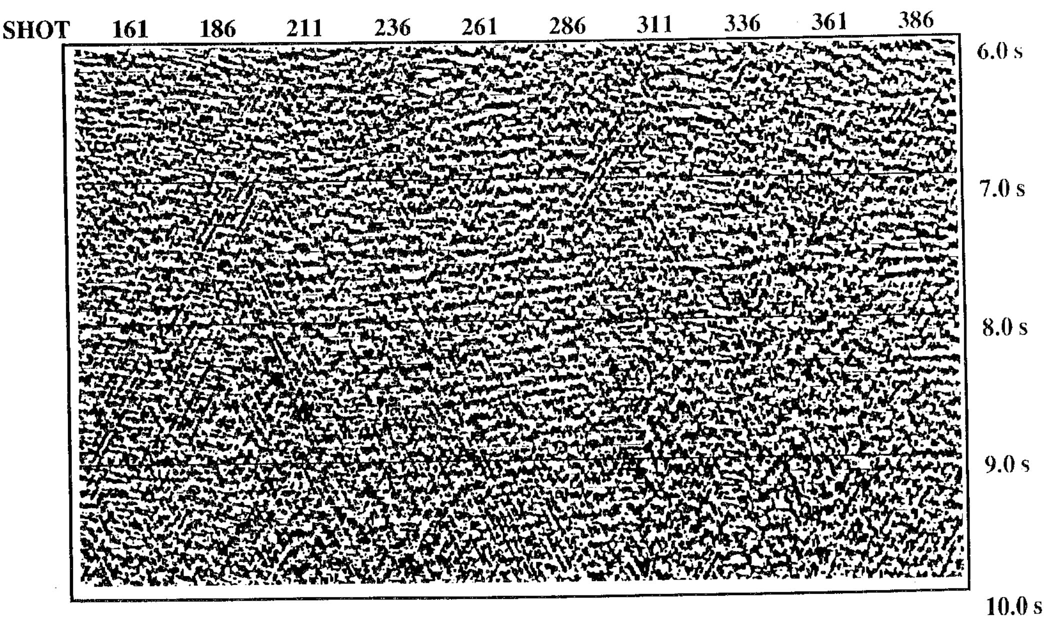

Fig. 6 — Line IT89A25: stack section of Fig. 5 after fx-deconvolution.

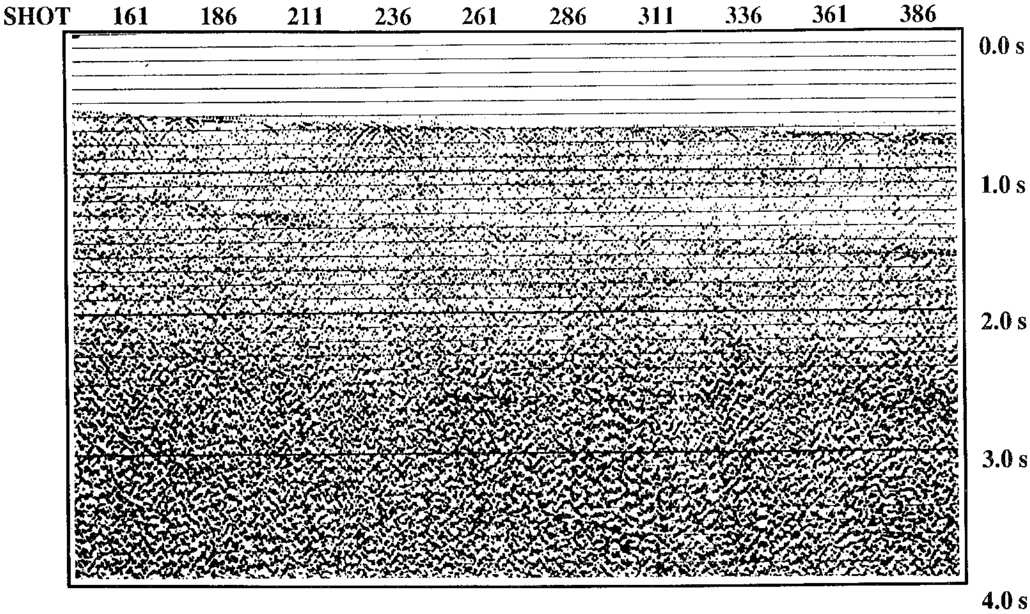

Fig. 7a —Line IT89A25: noise section of Fig. 6 (shallow part).

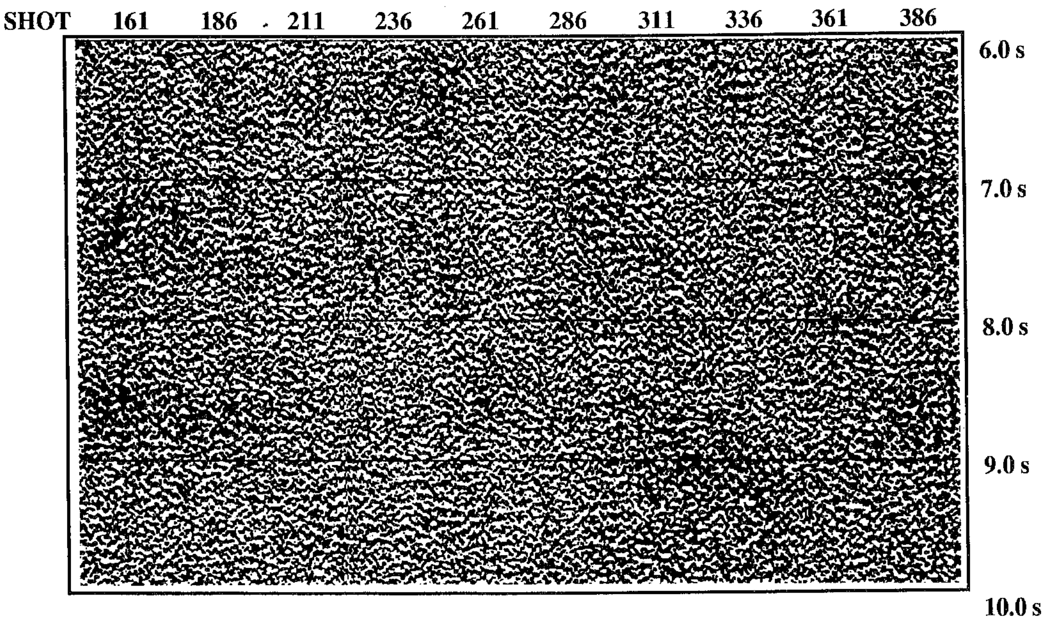

Fig. 7b — Line IT89A25: noise section of Fig. 6 (deep part).

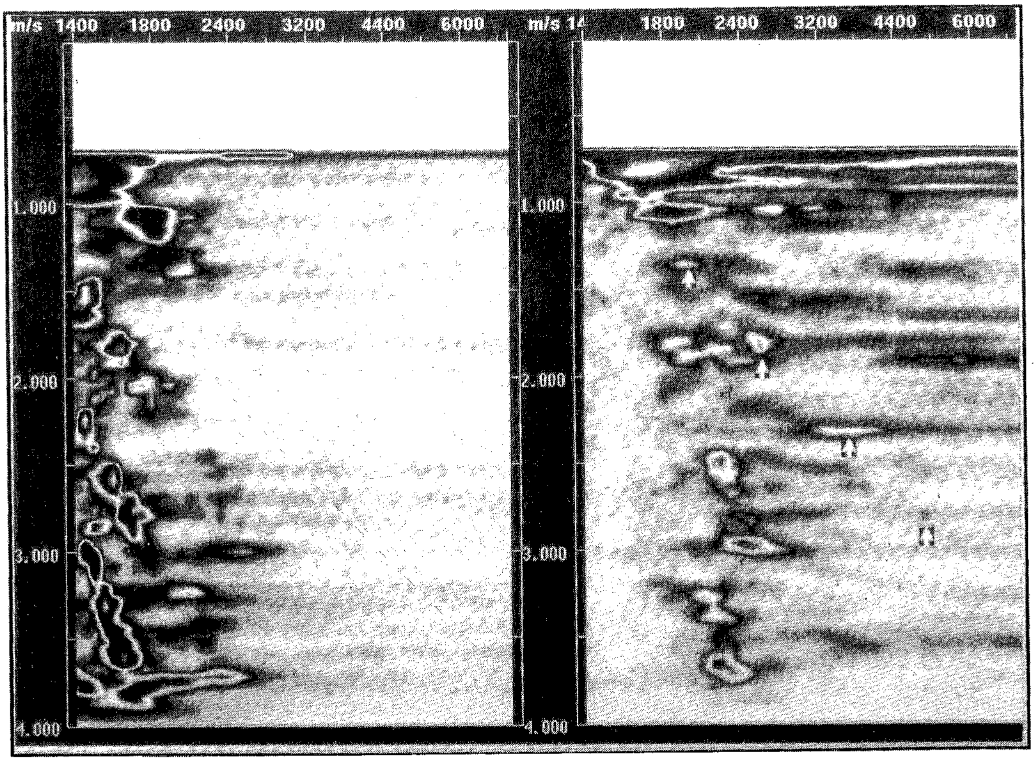

Fig. 8 — Line IT89A25: example of velocity spectra a) before and b) after the iterated application of fk fan filters.

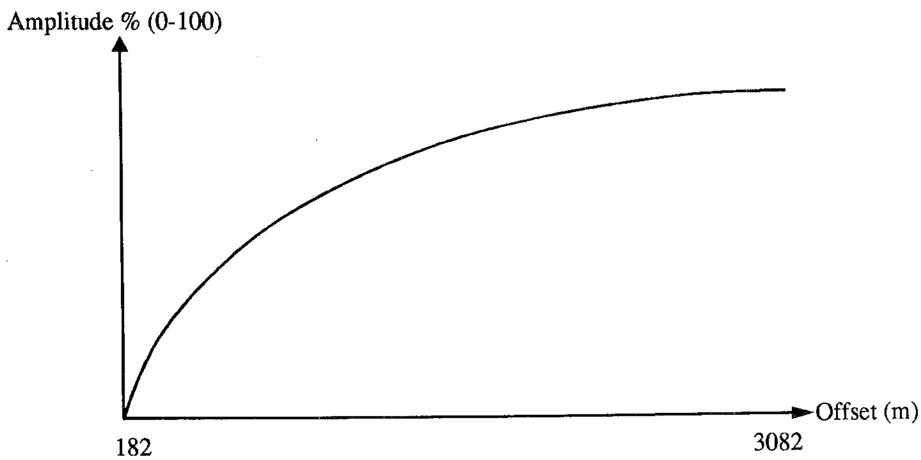

Fig. 9 — Example of weighting function employed in the weighted stack of the processed seismic sections.

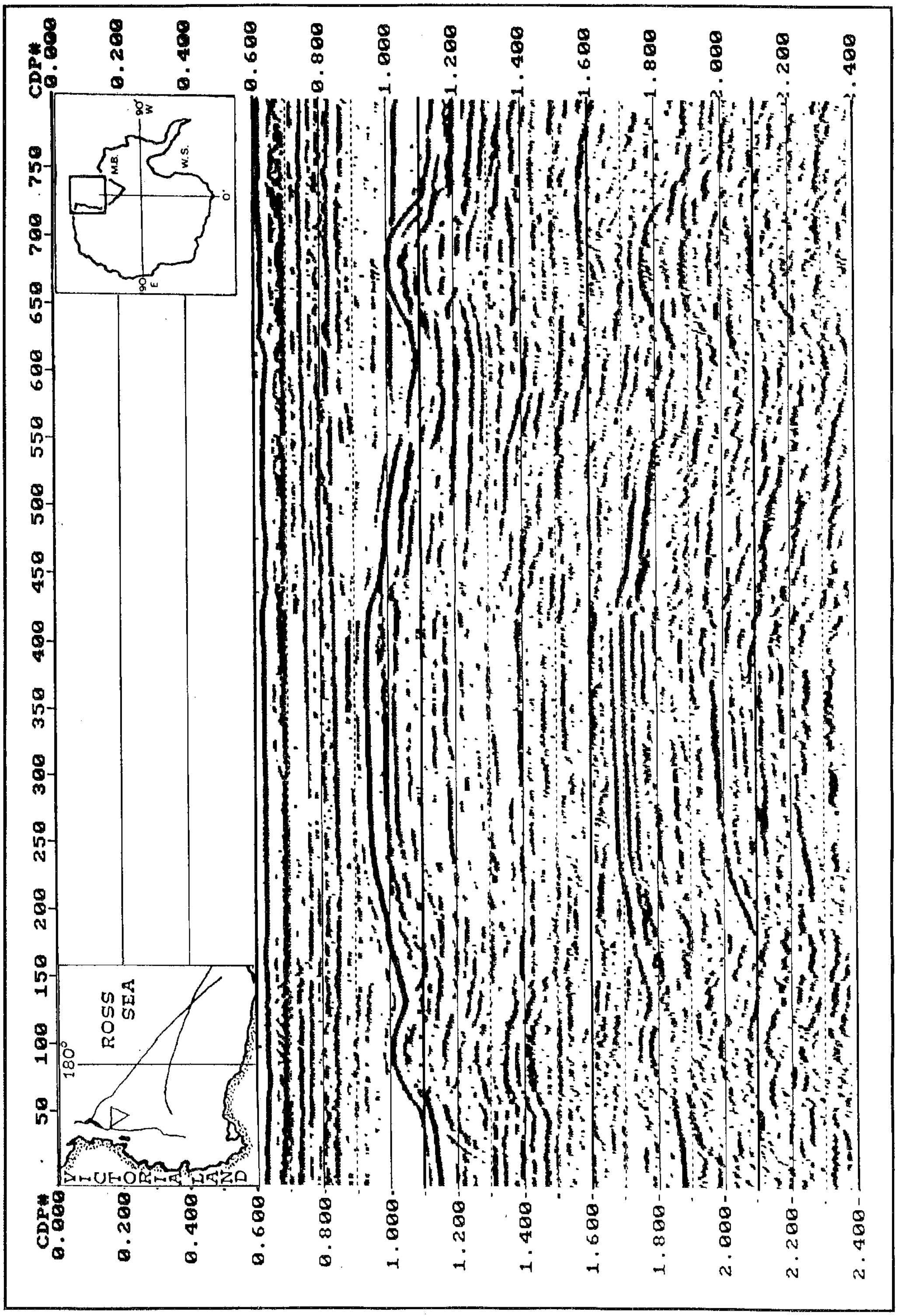

Fig. 10 — Line IT88A06: stack section after standard processing.

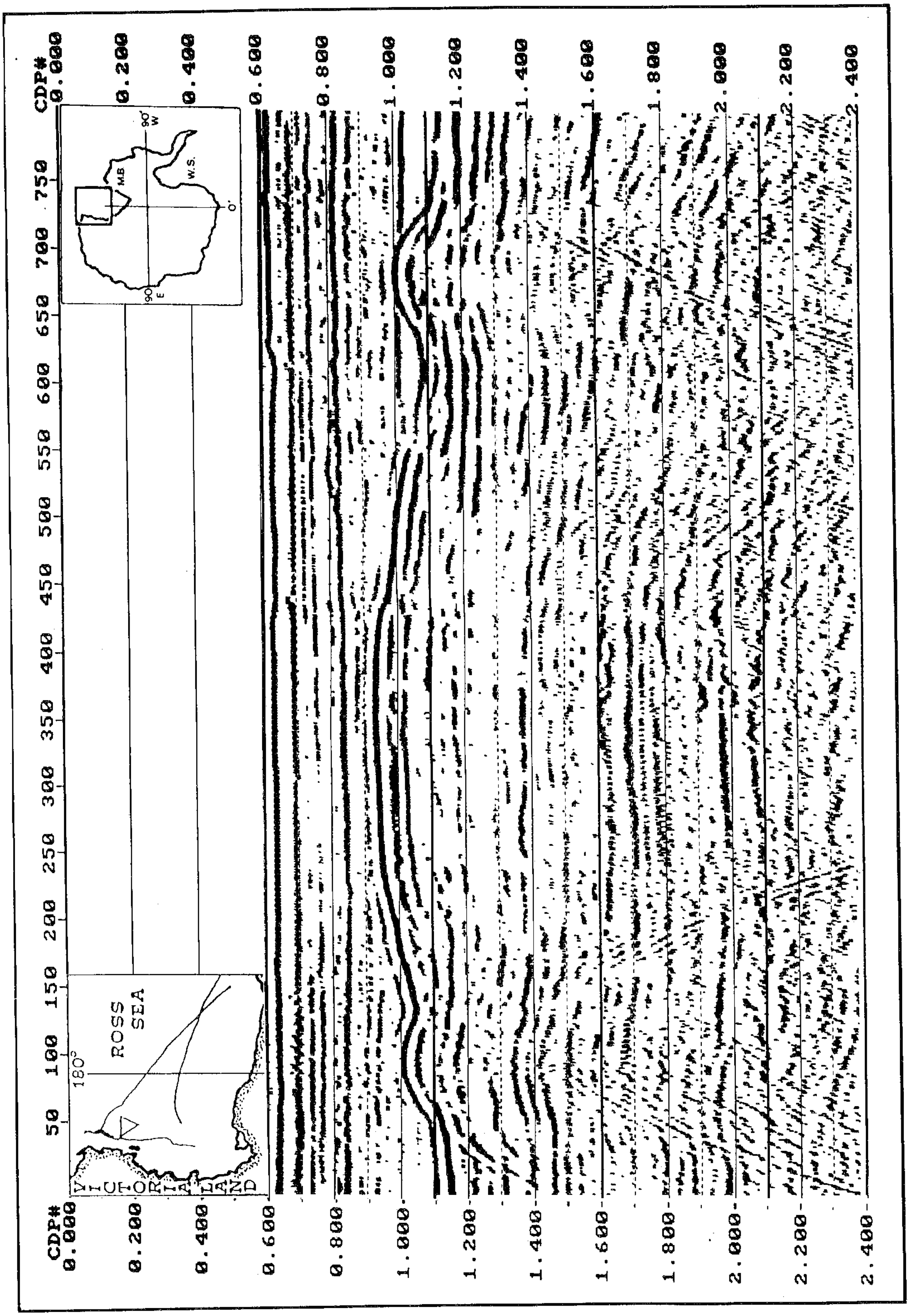

Fig. 11 — Line IT88A06: stack section after the iterated application of fk fan filters.

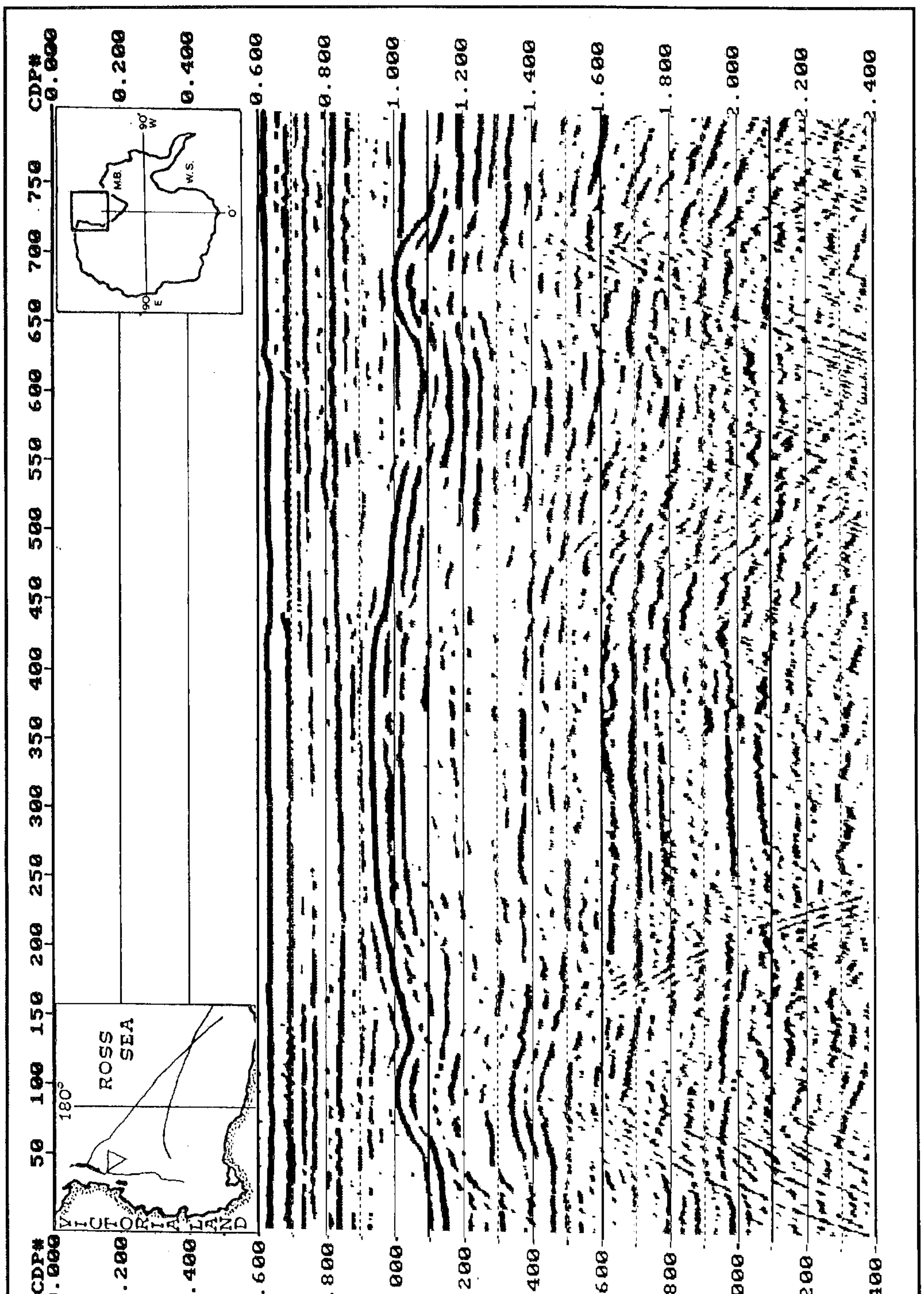

Fig. 12 — Line IT88A06: stack section of Fig. 11 plus fx-deconvolution after stack.

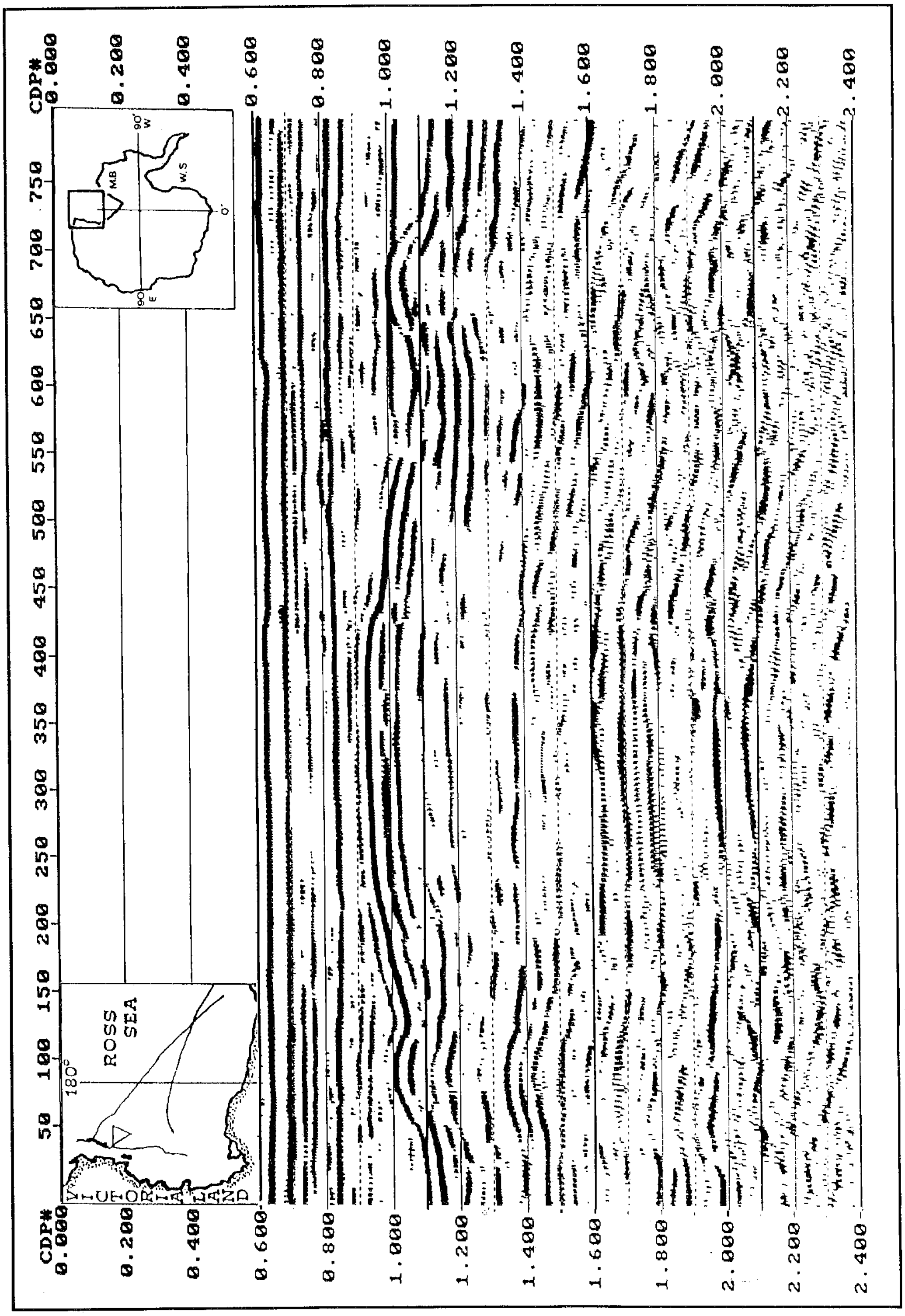

Fig. 13 — Line IT88A06: stack section of Fig. 11 plus fx-deconvolution before stack.

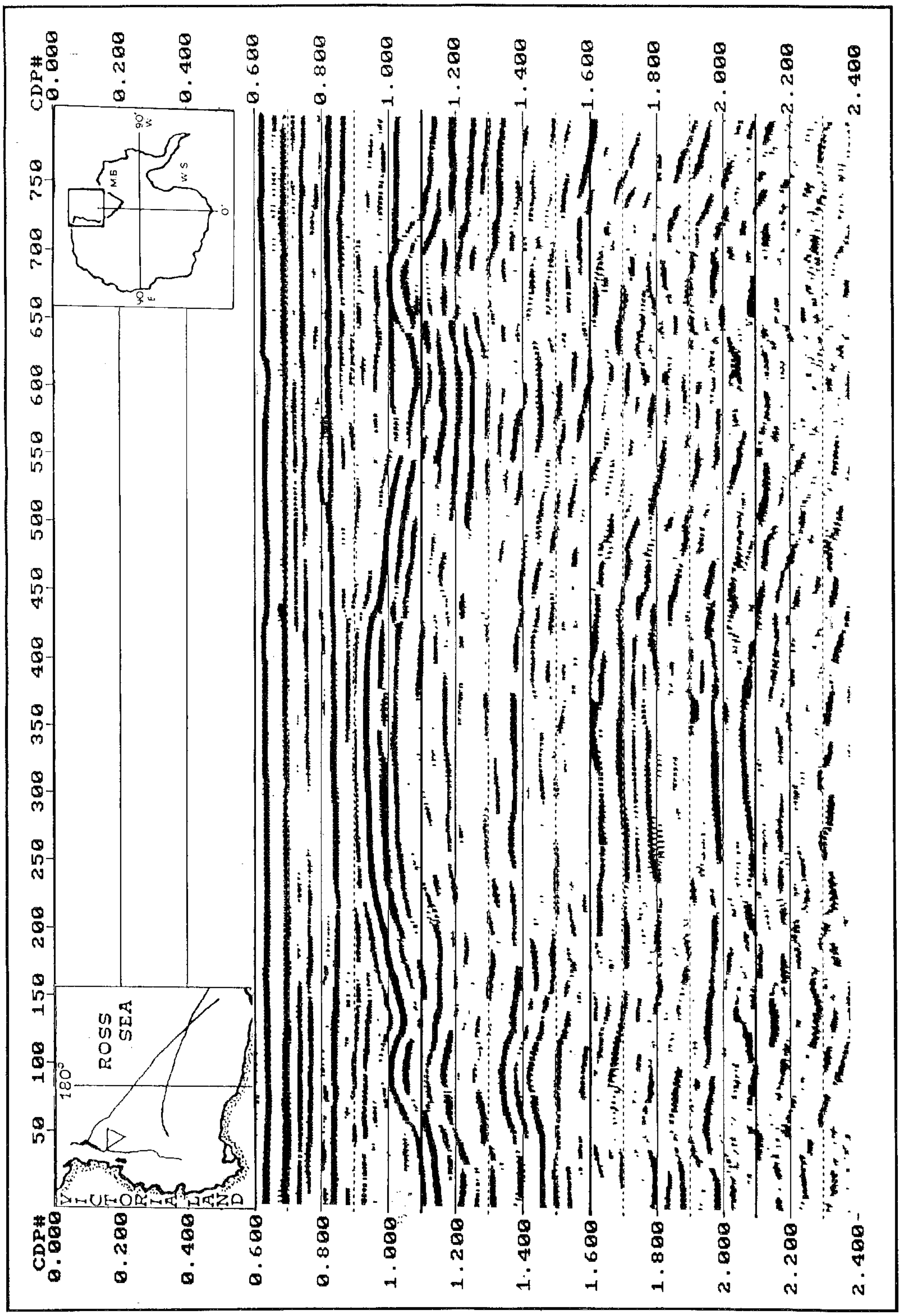

Fig. 14 — Line IT88A06: weighted stack section of Fig. 13.

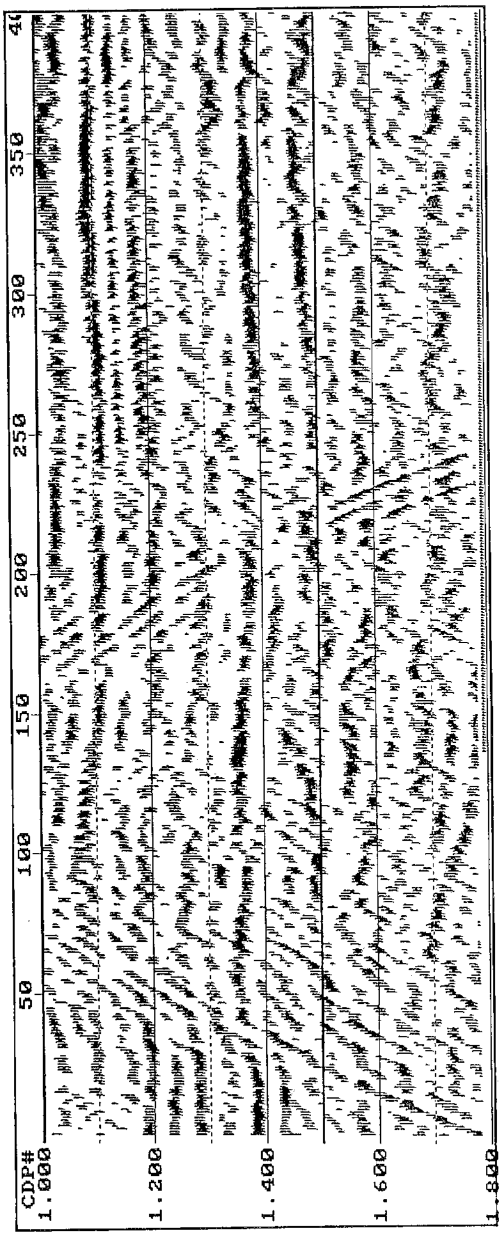

Fig. 15 — Line IT88A06: expanded detail of Fig. 10.

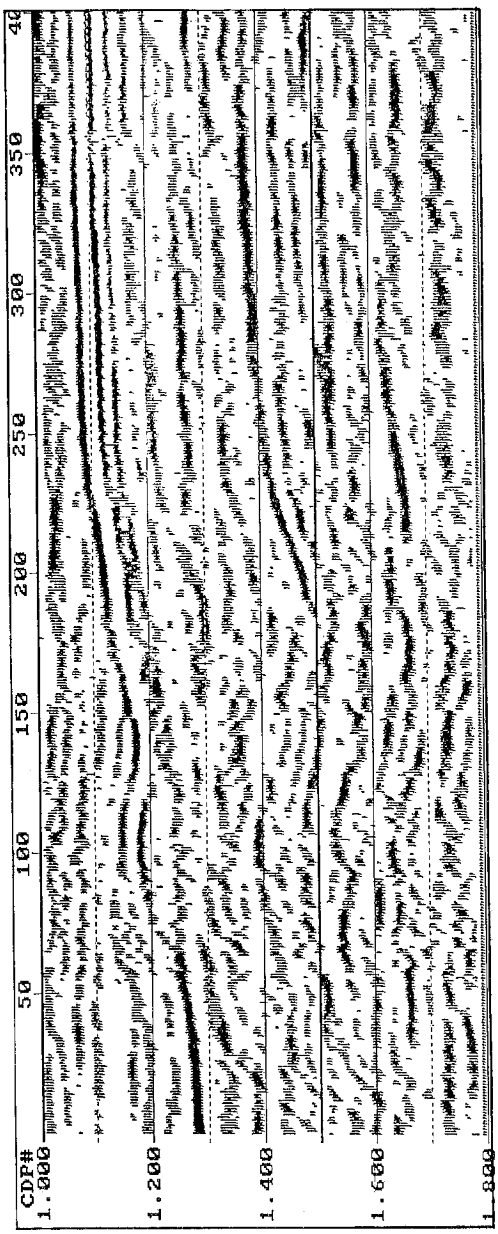

Fig. 16 — Line IT88A06: expanded detail of Fig. 11.

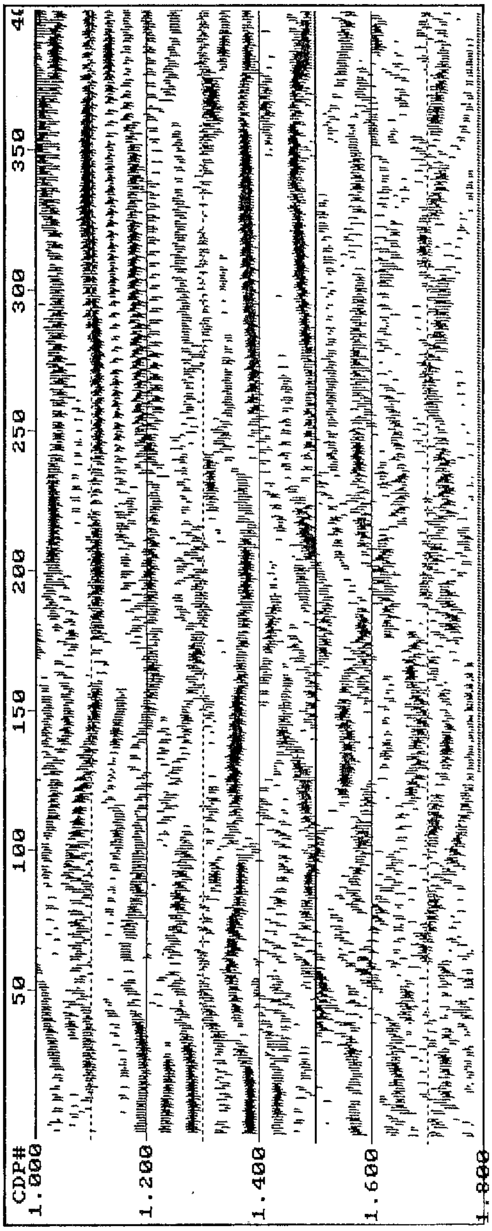

Fig. 17 — Line IT88A06: expanded detail of Fig. 12.

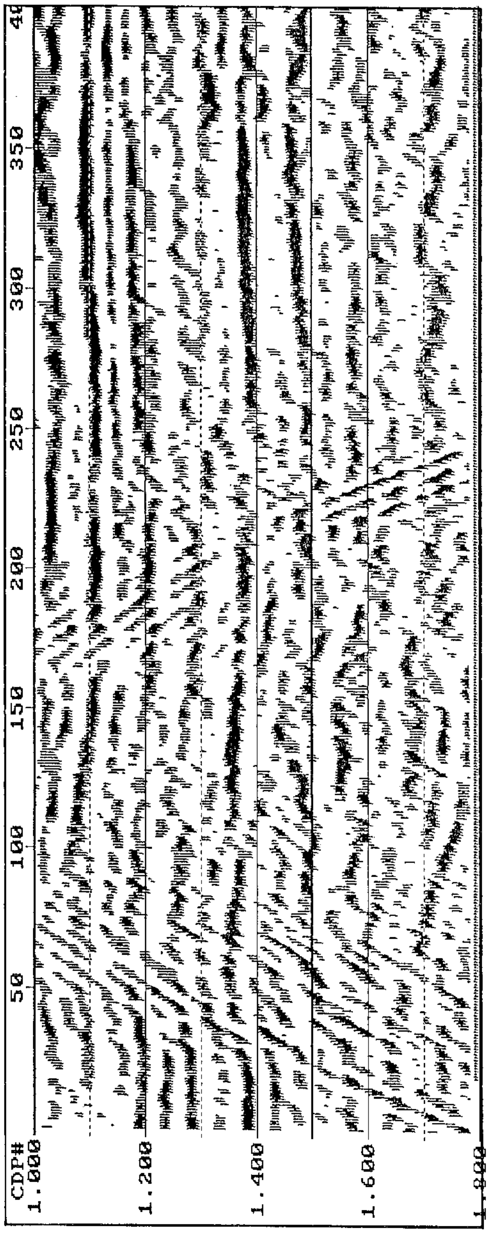

Fig. 18 — Line IT88A06: expanded detail of Fig. 13.

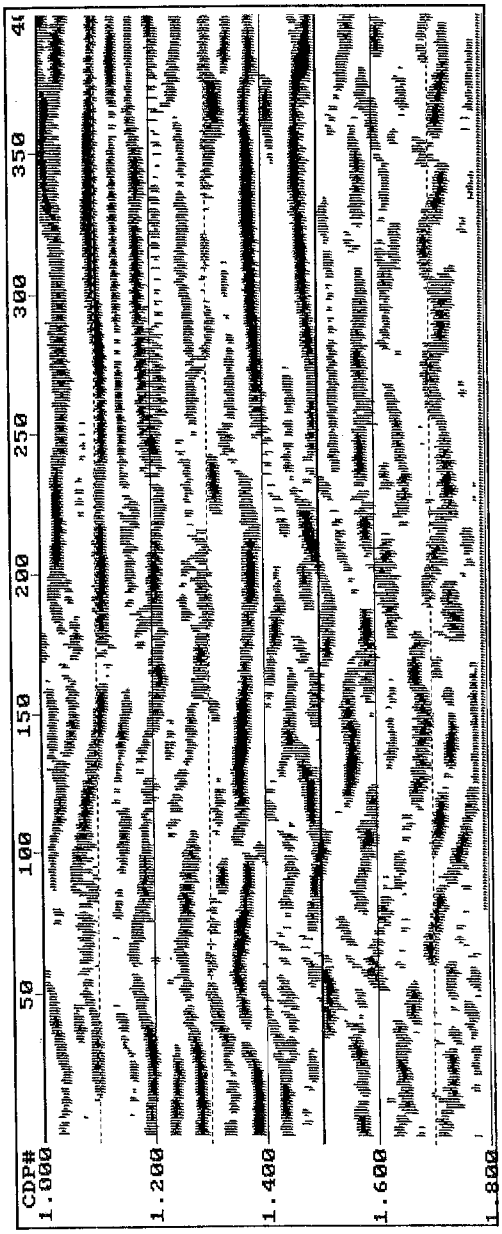

Fig. 19 — Line IT88A06: expanded detail of Fig. 14.

of a few years a very popular tool of seismic processing to enhance the signal noise ratio. This method allows a separation of the seismic data into two components: the spatially organized (the signal) and the uncorrelated one (the noise). Since the algorithm achieves its best performance when the data quality is not too poor, *f-x* deconvolution is typically applied to stacked sections.

The algorithm steps are the following:

- the seismic traces are converted into complex sequences in the frequency domain by a Fourier transform;
- for each arrival time, a complex sequence is extracted horizontally along the seismic section;
- a complex predictive deconvolution (Treitel,1974) is applied to such sequences, preserving the predictable part as the desired signal and rejecting the prediction errors as the unwanted noise;
- the filtered signal is converted back into the time domain.

The main advantage of the transform to the frequency domain is that in this way dipping events can be properly handled. In fact, coherent dipping signals are characterized by a regular (and therefore predictable) phase shift. Otherwise, without this transform, only sub-horizontal reflections would be enhanced.

F-x deconvolution differs from the more famous predictive deconvolution in various aspects, although they share the common philosophy that signal and noise can be separated by exploiting their different statistical properties. In the case of predictive decon, the useful signal is assumed to be the random component of the seismic trace, associated with the earth's reflectivity sequence; the noise is the predictable part, formed by the source and receiver signature and the multiples. *F-x* decon, on the contrary, assumes that the desired signal can be predicted laterally because of the usual spatial continuity of geological structures; the unorganized signal corresponds therefore to the ambiental noise or to scattered energy. This apparent disagreement stems from the different spatial dimensions in which the two techniques are applied: time (or depth) for predictive, distance along the profile for *f-x*. Both methods, in practice, assume almost the same earth model: homogeneous layers with parallel interfaces - not necessarily horizontal. A further hypothesis implicit in predictive deconvolution, i.e., that the velocity and thickness of layers correspond to a Goupillaud medium, is not necessary for *f-x* decon.

Figs. 10 and 12 display the results obtained applying a post- stack *f-x* deconvolution to the data in Figs. 6 and 7, respectively. We see a much clearer continuity of reflections, especially in the late arrivals. The effects of the *f-x* deconvolution are also illustrated by Fig.11, where the random noise that has been removed from the section by this procedure is displayed.

Both conventional stack and *f-x* deconvolution aim to enhance the signal noise ratio of the seismic traces by exploiting the spatial redundance of the collected data. For this reason, we decided to test the possibility of commuting the two procedures. In the prestack domain, there are four main data sort types which can be used: common shot, common receiver, common mid-point and common offset. The first three required a normal moveout correction with the exact stacking velocity to get an optimal lateral coherency, while this is not necessary for the last one. For this reason, we applied the *f-x* decon to common offset gathers, obtaining the results depicted in Fig.13. An almost identical result was obtained by NMO corrected CMP gathers. There is a noticeable improvement in the reflectors' continuity, particularly of those which were previously hidden by the multiples.

Although several deep primaries have been noticeably cleaned of random noise by *f-x* deconvolution, the spatially organized noise introduced by the previous f-k filtering was not removed at all. On the contrary, its high frequency content was increased. Since the noise is rather steep while the desired primaries are mostly sub-horizontal, a post-stack weighted mix was carried out: each trace in output had a small percentage (10 %) of the preceding and the following ones. In this way, a much clearer final image was produced (Fig.14).

CONCLUSIONS

The techniques and the results of the processing of seismic profiles recorded in the Ross

Sea have been presented and discussed. Since the conventional processing sequence was not able to reduce the strong multiple reflections from the frozen sea bottom, we used some special processing tools, such as weighted stack and iterated *f-k* domain pre-stack filtering, obtaining a satisfactory attenuation of multiples. The weak underlying deep primaries were finally enhanced by a new technique, pre-stack *f-x* deconvolution of the common offset gathers.

The seismic sections finally obtained display clearly several deep reflectors which were almost uninterpretable on the images produced by a conventional processing. A considerable overall improvement in the processed sections shows up along the whole span of the records, as can be observed on enlarged details of the stacked sections previously considered (Figs. 15 to 19).

REFERENCES

Gulunay, N.; 1986: *FXDECON and complex Wiener prediction filter*. In: Expanded Abstracts of the 56th SEG Meeting, pp. 279-281.

March, D.W. and Bailey, A.D.; 1983: *A review of the two- dimensional transform and its use in seismic processing*. First Break.

Treitel, S.; 1974: *The complex Wiener filter*. Geophysics **34**, 155-169.